Two Benchmarks for the Study of Compact Thermal Modelling Phenomena

Clemens J.M. Lasance
Philips Research Laboratories
Prof. Holstlaan 4, 5656 AA Eindhoven, The Netherlands
clemens.lasance@.philips.com

Abstract

The paper discusses two benchmark cases to facilitate the study of compact thermal models. The benchmarks represent idealised concepts of respectively a leaded package (PFQP-style) and an area-array package (BGA-style). Two different boundary conditions sets are included because both package types require such. The objective of the paper is to formulate a framework that can be used by everyone working in the field. In this way, comparison of results emerging from alternative approaches in defining compact models becomes much easier. In this paper only steady state models are discussed, but the benchmarks are also developed for dynamic modelling research purposes.

Introduction

Since the publication of the first paper on boundary-condition-independent (BCI) compact thermal models by the DELPHI consortium (Lasance et al., 1995), the concept has attracted wide attention because of its potentially high accuracy. These models enable the system level designer to predict the temperature of potentially critical components with the accuracy required for reliability prediction, without knowing all the details of the component in question.
The following procedure highlights the procedure used to arrive at compact models:

1. Creation of a 'full' model of an electronic device. This 'full' or detailed model can be made with any type of software package.
2. A usually large set of combinations of boundary conditions, representing all conditions that a device may encounter in practice, is imposed on all faces where significant heat transfer occurs. The junction temperature and heat flow rate through each side is then calculated, using the full model for all boundary conditions.
3. Definition of a cost function which is to be minimised in the optimisation procedure.
4. Definition of a thermal network, i.e., the 'compact model', which should be able to characterise the thermal behaviour of the package. When a surface of a package has to be sub-divided, the area ratio is also a parameter in the optimisation.
5. The actual optimisation. By varying the thermal links in the net-work, the user-specified cost function is minimised. When the results are within the required accuracy range, a compact model that is 'independent' of the imposed boundary conditions is obtained.

The emphasis is on the phrase 'boundary-condition-independent'. The following subsection treats this subject in some detail.

1. On Boundary-Condition-Independence and Division of Responsibilities

Some controversy exists about the precise meaning of BCI. The question when to call a compact model BCI cannot be answered in a unique way. Based on experience with many package types, we propose the following definition:

A compact model is a BCI model if the relative difference between compact and detailed model data with respect to the parameters constituting the objective function, such as junction temperature and heat fluxes does not exceed a certain agreed percentage for an agreed set of boundary conditions.

For example, the thermal community could agree on 10%. A 'full' or 'detailed' model of the package only is per definition BCI, because the model itself does not include any influence of whatever boundary condition. On the other side of the spectrum, a model with only one parameter, for example a model defined by a measurement of the junction-to-case thermal resistance, is definitely not BCI, because this value changes as a function of the applied boundary condition.

The main advantage of BCI models is that they allow for the first time a separation of responsibilities between vendor and customer. This goal cannot possibly be realised using the currently popular thermal metrics such as R_{TH-JA} or R_{TH-JC}, because these metrics depend on the type of measurement chosen by the vendor. In this light, the *formal responsibilities of the component vendor* could be stated as:

- Creation of detailed (preferably parameterised) thermal models.
- Experimental validation of these models.
- Publication of an ASCII file with $T_{junction}$ and heat flux data for a well-defined set of boundary conditions. For example, such a file could be published on the web and downloaded by certified customers. This approach provides all data for the creation of arbitrary compact models, yet provides no detailed information about the package itself.
- Measurement of standardised metrics such as R_{JB} and R_{JC}, only for the purpose of comparison. It can be envisioned that this step can be abandoned at some moment in future.

The *customer's responsibility* is:

- The creation of compact models with the required degree of complexity depending on the application and the software in use. Both star-models and BCI-models can be generated in a matter of minutes using dedicated software.

In order to be widely accepted, the thermal community has to agree on a number of issues which are still under dispute: the (minimum) number of boundary conditions, their values, the cost function, the optimal statistical optimisation strategy, the way the compact model is represented, etc.

Another important issue that is highly relevant for the EC-funded PROFIT project (PROFIT, 2000), is the study of dynamic phenomena. To guide these studies, we need benchmarks providing detailed model data that can be used by everyone to facilitate comparison of results. This paper describes such benchmarks.

2. The Proposed Benchmarks

Suitable benchmarks can be constructed by defining idealised packages, preserving the most important details of a real package, but lacking their complexity. The advantage over real packages is simply the reduction in calculation time. In practice, running a detailed (and validated) model of a real package poses no problem when the objective is only to construct a compact model, given a certain boundary condition set, cost function etc. that has been agreed upon, because only one run is sufficient. However, when the objective is to study these topics, the issue of speed becomes important.

The reason for selecting these benchmarks is that they represent simplifications of the two most popular package styles: the first represents a leaded package (TQFP-like), the second an area-array package (BGA-like). It was decided that selecting only one benchmark neglects the fact that the heat transfer paths, given certain boundary conditions, are very different for the two styles. Hence, a compact modelling approach that could work for one style, might fail for the other.

Appendix A contains a detailed description of all relevant dimensions and physical properties of both benchmarks, while Fig. 1 shows the layouts. The chosen dimensions and material properties are typical for current packages, and the dimensions of the various parts (die, die pad, etc.) are chosen to facilitate simulation, especially mesh generation.

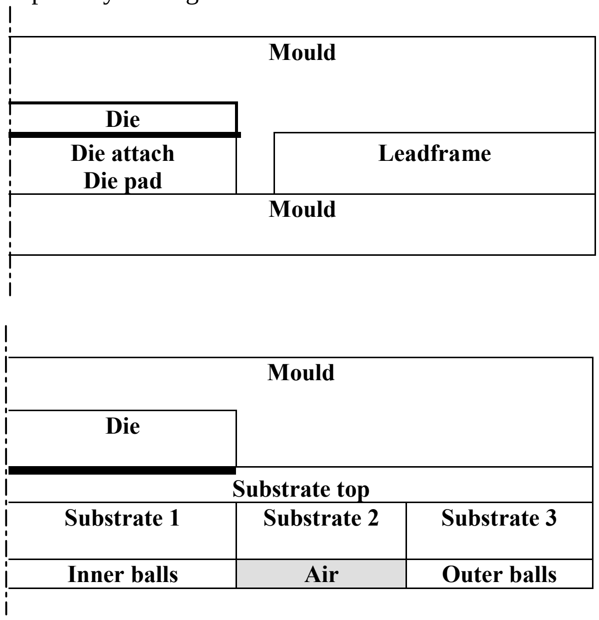

Figure 1. Sketches of TPFP (top) and BGA (bottom). Quarter symmetry.

3. Benchmarking the Benchmarks

It is always highly recommended to check numerical models on possible errors in modelling and on the grid that is required to achieve a certain level of accuracy. By changing a number of dimensions and properties in such a way that a stack of layers with uniform properties per layer results, we have tested the benchmark cases against analytical solutions, such as provided by commercially available software (THERMAN, 1999).

In order to ascertain that grid independence is realised in all directions and for all possible boundary conditions, a special set of boundary conditions was used representing essentially the DELPHI DCP1-4 boundary conditions (see e.g. Pape and Noebauer, 1999). The purpose of these experimental boundary conditions is to force the heat through all the areas of interest one by one. Also the 'infinite' boundary condition has been added to the list. Table 2 shows the set used.

A difficulty was encountered in defining the boundary conditions for the BGA, due to the fact that the 'bottom' of the package is not in the same plane as the ball areas (see shaded area in Fig.1). This is not a problem as long as the package is mounted on a board or cold plate, because then the air layer plays a role, but it is for the fluid bath and DCP boundary conditions. In order to prevent possible sources of misunderstanding, it has been decided to define all boundary conditions at the bottom at the same plane, z=0. However, for the BGA DCP2 boundary condition we ran into another problem, because two very different boundary conditions are applied at the same plane comprising two very different materials. We face a singularity at the corners of the interface between air and the ball areas. Besides, it is also technically impossible to impose two different boundary conditions at one point. We were able to solve this problem by imposing the bottom condition on an area reduced by 0.1 mm at all sides.

Table 2 *Boundary conditions (values for h in W/m^{2}K) to check grid independence*

#	*b.c.*	*Top*	*Bottom*	*Side*	*Leads*
1	*DCP-1*	10000	10000	1	1
2	*DCP-2*	10	10000	1	1
3	*DCP-3*	10000	10	1	1
4	*DCP-4*	1	1	1	10000
5	*Infinite*	10^9	10^9	10^9	10^9

The author uses proprietary software (Pstar, a SPICE-like software code) because it allows the user the generation of detailed model data for all boundary conditions of interest in a very easy way. The optimal grid was found by comparing the results for the five test boundary conditions shown in table 2 against a Flotherm conduction-only model with a very fine grid (which itself was tested on grid-independence), and a FEM model built using MARC. The comparison resulted in the following table. For reasons of convenience, the BGA data shown in Table 3 are calculated for the ***isotropic*** case, for which the thermal conductivities are uniform in all directions. After benchmarking, the ***anisotropic*** data for the boundary conditions sets reproduced in Appendix B have been generated using Pstar. These data are to be considered as the benchmark data, and can be found on the PROFIT website.

Table 3 *Comparison of calculated junction-to-ambient thermal resistances for various software, for the boundary conditions of Table 2,* ***isotropic thermal conductivities.***
*TQFP: Flotherm fine (44*44*26, linear elements), finer (87*87*38), MARC (7689 quadratic elements), Pstar coarse (12*12*8).*
*BGA: Flotherm coarse (17*17*14), fine (33*33*33), MARC (15000 quadratic elements), Pstar coarse (13*13*10).*

TQFP				
# b.c.	***Flotherm***		***MARC***	***Pstar***
	fine	***finer***	***fine***	***coarse***
1	4.31	4.26	4.21	4.35
2	6.76	6.67	6.57	6.87
3	7.32	7.21	7.10	7.45
4	24.21	23.48	22.92	25.13
5	3.82	3.78	3.74	3.85
BGA (Isotropic)				
# b.c.	***Flotherm***		***MARC***	***Pstar***
	coarse	***fine***	***fine***	***coarse***
1	5.91	5.72	5.75	5.85
2	35.30	34.70	36.8	35.11
3	5.86	5.76	5.82	5.95
4	1.63	1.63	1.63	1.63
5	0.677	0.678	0.68	0.680

Table 4 *Comparison of calculated junction-to-ambient thermal resistances for various software, for the boundary conditions of Table 2,* ***anisotropic thermal conductivities.***
*BGA: MARC (15000 quadratic elements), Pstar coarse (13*13*10).*

BGA (Anisotropic)		
# b.c.	***MARC***	***Pstar***
	fine	***coarse***
1	5.94	6.04
2	37.57	36.54
3	6.02	6.13
4	2.01	2.02
5	1.04	1.04

The rather high value for BGA DCP2 case requires some explanation. Looking at the sketch of the BGA, you will notice that the ball and bottom areas are not in the same plane. For reasons of convenience, we have chosen to define the boundary conditions for both areas at the same plane, z=0. However, the result is that an air layer is always present between the bottom and the bottom boundary condition plane. In nearly all cases no problem are expected, the exception being DCP2 in which all the heat is forced through the bottom area. We learned also an important lesson: it took us a lot of time before we could conclude that mesh independence was achieved. It appeared very important to employ strongly non-equidistant grids, concentrating grid lines in areas of very high temperature gradients. Even for this relatively small volume, 'standard' mesh generation would require more than 300.000 cells. For all other boundary conditions, the accuracy using the coarse grid is considered sufficient given the reduction in speed (order of magnitude 50 times).

4. The Proposed Boundary Condition Set

Lasance et al. (1999) proposed a new set (the '99' set) to replace the '38' set that has also been used by many other research groups involved in compact modelling. While the '38' set provides the same accuracy as the '99' set, the last set has a number of advantages. First, because the set is much larger, one has the opportunity to select a certain subset (for example natural convection only, with and without heat sinks), that still comprises enough boundary conditions for subsequent optimisation. Second, the set shows symmetry: for some packages, it is possible to mount them both ways, for other packages such as BGA's this is not possible. A last advantage of the larger set is that it allows cross-validation: a compact model is created using say 50 boundary conditions, and the remaining boundary conditions are used to check the validity of the model. An alternative method that is better but more time-consuming is to optimise for n-1 boundary conditions, check the model for the n-th boundary condition, and repeat this procedure for all combinations. This will be part of future research by CQM.

The published '99' set was developed for leaded packages, which becomes obvious by observing the rather high values for the heat transfer coefficients associated with the leads. The reason is simply that the cross-sectional area of the leads is very small, and the combination leads-board acts in fact as a fin, enlarging effectively the area and thus the heat transfer coefficient. Such is not the case for area-array packages, because the areas representing the 'leads' (more precise, the balls) are much larger. Hence, a special boundary condition set was constructed for the BGA benchmark. Both sets are reproduced in Appendix B.

5. Results with Pstar/OPTIMIZE

The results in this section have been calculated using Pstar/OPTIMIZE and DOTCOMP. Both for the TQFP and the BGA, the five last 'unrealistic' boundary conditions have not been used in the optimisation, although adding them did hardly affect the results. The following definition of the cost function has been used:

$$\frac{1}{BC}\sum_{i=1}^{BC}\left[V\left(\frac{T_{i,c}-T_{i,f}}{T_{i,f}-T_{amb}}\right)^2+\frac{W}{N}\sum_{i=1}^{N}\left(\frac{\Phi_{i,f}-\Phi_{i,c}}{\Phi_{total}}\right)^2\right]$$

,

where subscripts c and f denote 'compact' and 'full' respectively, BC is the number of boundary conditions, N the number of faces, and V and W weight factors. V has been added to allow comparison with optimisation software allowing only the fluxes to be optimised, by setting the value to zero. Using DOTCOMP, an optimal value for W can easily be found. The only function of BC and N is that adding them allows comparison of the cost function value between runs using different values for BC and/or N.

TQFP

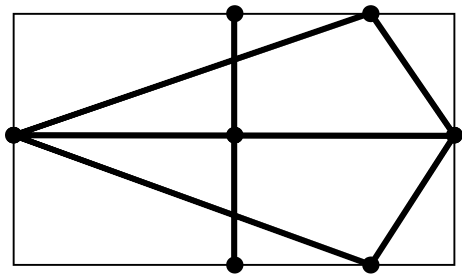

Links	*K/W*	*Error percentages*	
j-t1	41.1	**Tmax**	**Φmax**
j-b1	37.5	1.5	3.6
j-s	142		
j-l	151	**Cost function**	
t2-l	16.4	$6.0\ 10^{-7}$	
t2-s	4.36		
b2-l	24.7		
b2-s	10^{-5}		
	-		
par	0.164		

Figure 2 The sketch shows the location of the nodes with the junction in the centre. The table shows the values for the indicated links between the nodes. The parameter 'par' represents the optimised area ratios allocated to both the top and bottom nodes.

BGA (Anisotropic)

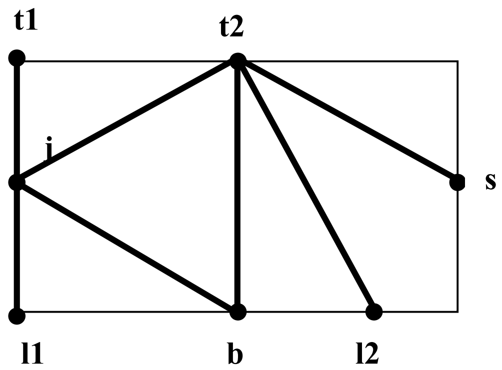

Link	K/W	Error percentages	
j-t1	37.6	Tmax	Φmax
j-l1	5.14	1.9	5.1
j-t2	72.9		
j-b	555	Cost function	
t2-b	588	$2.8\ 10^{-5}$	
t2-l2	1.30		
t2-s	59.8		
	-		
partop	0.103		
parleads	0.074		

Figure 3 The sketch shows the location of the nodes with the junction to the left. The table shows the values for the indicated links between the nodes. The parameter 'partop' represents the optimised area ratio allocated to the top nodes, 'parleads' the ratio to the leads nodes.

Note that the error percentages are defined according to the formulation in the cost function. It is interesting to observe that the optimised area ratio for the BGA lead areas is approximately equal to the real ratio, which is 0.077. Normal practice would indeed be to fix the real ratio, instead of optimising it.

6. Future Research

All groups that are involved in compact model research have been invited to use the proposed benchmarks to generate compact models using the boundary condition sets and prescribed cost functions. The main goal is to evaluate the various methods that are currently in use to minimise the cost function, such as least squares, genetic algorithms and nonlinear programming, hopefully resulting in recommendations for a most suitable compact modelling practice. The results will be published in a future paper. People who want to join or to use the boundary conditions are encouraged to contact the author, or download the required files from the PROFIT website.

Conclusions

Two idealised packages representing respectively a TQFP and a BGA have been described to be used as benchmarks for the study of various compact modelling topics. The full models show sufficient detail to make them suitable for parametric studies, yet do not require computationally extensive runs. However, it was also found that extreme care is required to reach grid independence. This is considered an important point when it comes to validation of detailed models, using experiments that generate large temperature gradients. Results are presented for compact models of both benchmark cases. Suggestions are given to make optimal use of the proposed benchmarks.

Acknowledgments

The author appreciates the contributions of John Janssen (Philips Semiconductors, also for providing detailed model data), John Parry (Flomerics), and Claudio Maria Villa (ST Microelectronics) in defining the most suitable formulation of the two benchmarks. Also, the partial support of the European Community under the IST contract PROFIT is acknowledged.

REFERENCES

Lasance C., Vinke H., Rosten H., Weiner K.-L., 1995, *A Novel Approach for the Thermal Characterization of Electronic Parts*, Proc. of SEMITHERM XI, San Jose, CA, pp. 1-9.

Lasance C., den Hertog D., Stehouwer P., 1999, *Creation and Evaluation of Compact Models for Thermal Characterisation Using Dedicated Optimisation Software*, Proc. of SEMITHERM XV, San Diego, CA, pp. 189-200

Pape H., Noebauer G., 1999, *Generation and Verification of Boundary Condition Independent Compact Thermal Models for Active Componenta According to the DELPHI/SEED Methods*, Proc. of SEMITHERM XV, San Diego, CA, pp. 201-211

PROFIT:
www.extra.research.philips.com/euprojects/profit/

THERMAN: www.micred.com

APPENDIX A PROPERTIES OF THE TWO BENCHMARKS

Dimensions and Thermal Properties of the TQFP Benchmark

TQFP Benchmark (Quarter Symmetry)			
dimensions (mm)	*10*10*1.42*	*Dissipation (W)*	0.25
die size (mm)	*4*4*	*Also die attach and die pad 4*4*	
gap (mm)	*0.2*	*Source covering whole top of die*	
width frame (mm)	*5.8*		
Layer	**Thickness (mm)**	**Thermal conductivity (W/mK)**	**Thermal capacity (J/m3K)**
*mould (top, **above die**)*	0.5	0.75	2.0e+6
die	0.3	100	1.5e+6
die attach	0.02	1	2.0e+6
lead frame	0.2	200	1.5e+6
mould (bottom)	0.4	0.75	2.0e+6
Die paddle	0.2	380	3.0e+6
Gap die/frame	0.2	0.75	2.0e+6

***Note*: observe that the mould thickness at the top of the package is defined from the top of the die onwards.**

Note: if possible, use also the following temperature dependent thermal conductivity for Si:
k = 150*(T/300)**-4/3, with T in K. Especially recommended for time-dependent studies.

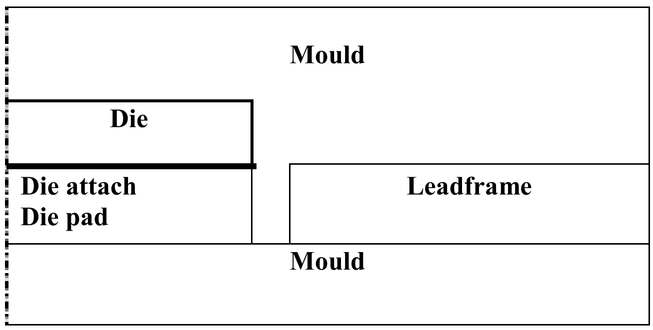

***Note**:* This benchmark can be checked against an analytical solution such as provided by e.g. THERMAN by equalising the thermal conductivities of die pad and leadframe, of the die and part of the mould adjacent to it, and deactivating the die attach.

Dimensions and Thermal Properties of the BGA Benchmark

BGA Benchmark (Quarter Symmetry)			
dimensions (mm)	*20*20*2.15*	*Dissipation (W)*	0.25
die size (mm)	*5*5*	*Source covering whole top of die*	
substrate 1	*5*5*		
substrate 2	*5*10*	*(L-shape)*	
substrate 3	*10*20*	*(L-shape)*	
inner balls (mm)	*5*5*		
air	*5*10*	*(L-shape)*	
outer balls (mm)	*10*20*	*(L-shape)*	
Layer	**Thickness (mm)**	**Thermal conductivity (W/mK)**	**Thermal capacity (J/m3K)**
*Mould (top, **above die**)*	0.7	0.6	2.0e+6
die	0.3	100	1.5e+6
die attach	0.02	1	2.0e+6
substrate top	0.03	200	3.0e+6
substrate 1	0.6	In-plane: ***20*** Thru: 8	2.0e+6
substrate 2	0.6	In-plane: ***5*** Thru: 2	2.0e+6
substrate 3	0.6	In-plane: ***10*** Thru: 4	2.0e+6
air	0.5	0.03	1.0e+3
inner balls	0.5	In-plane: ***0.05*** Thru: 25	1.0e+6
outer balls	0.5	In-plane: ***0.05*** Thru: 25	1.0e+6

***Note*: observe that the mould thickness at the top of the package is defined from the top of the die onwards.**
***Note*: the thermal conductivities used in the *isotropic* calculations are indicated in bold italic.**

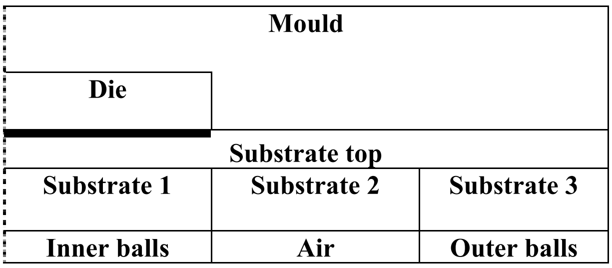

Note: This benchmark can be checked against an analytical solution such as provided by e.g. THERMAN, by equalising:

1. the thermal conductivity of the air to that of the solder balls,
2. the substrate thermal conductivities,
3. the thermal conductivity of the die to that of the mould adjacent to it,
4. deactivating the die attach.

Ambient temperature for temperature dependent thermal conductivity runs: 20 °C

Note: using analytical solutions, most software allows for either constant temperature or adiabatic boundary conditions at the sides. For this purpose, table 2 should be adapted by changing 1 to 0 for the sides and leads (PQFP) and sides only (BGA).

APPENDIX B
THE '99' TQFP AND THE '58' BGA BOUNDARY CONDITION SETS

The 99 Boundary Condition Set for the TQFP Benchmark

No		α_{TOP} W/m^{2}K	α_{BOT} W/m^{2}K	α_{SIDE} W/m^{2}K	α_{LEADS} W/m^{2}K
1	**A**	5	1	5	100
2		5	10	5	1000
3		5	50	5	1000
4		5	50	5	4000
5		5	100	5	1000
6		5	100	5	500
7		15	1	15	100
8		15	10	15	1000
9		15	50	15	1000
10		15	50	15	4000
11		15	100	15	1000
12		15	100	15	500
13		1	5	5	100
14		10	5	5	1000
15		50	5	5	1000
16		50	5	5	4000
17		100	5	5	1000
18		100	5	5	500
19		1	15	15	100
20		10	15	15	1000
21		50	15	15	1000
22		50	15	15	4000
23		100	15	15	1000
24		100	15	15	500
25	**B**	30	5	30	500
26		30	30	30	3000
27		30	200	30	10000
28		30	500	30	2000
29		80	5	80	500
30		80	30	80	3000
31		80	200	80	10000
32		80	500	80	2000
33		200	5	200	500
34		200	30	200	3000
35		200	200	200	10000
36		200	500	200	2000
37		5	30	30	500
38		200	30	30	10000
39		500	30	30	2000
40		5	80	80	500
41		30	80	80	3000
42		200	80	80	10000
43		500	80	80	2000
44		5	200	200	500
45		30	200	200	3000
46		500	200	200	2000
47	**C**	25	1	5	100
48		25	10	5	1000
49		25	50	5	1000
50		25	50	5	4000
51		25	100	5	1000
52		25	100	5	500
53		75	1	15	100
54		75	10	15	1000
55		75	50	15	1000
56		75	50	15	4000
57		75	100	15	1000
58		75	100	15	500
59		1	25	5	100
60		10	25	5	1000
61		50	25	5	1000
62		50	25	5	4000
63		100	25	5	1000
64		100	25	5	500
65		1	75	15	100
66		10	75	15	1000
67		50	75	15	1000
68		50	75	15	4000
69		100	75	15	1000
70		100	75	15	500
71	**D**	150	5	30	500
72		150	30	30	3000
73		150	200	30	10000
74		150	500	30	2000
75		500	5	200	500
76		500	30	200	3000
77		500	200	200	10000
78		500	500	200	2000
79		5	150	30	500
80		30	150	30	3000
81		200	150	30	10000
82		500	150	30	2000
83		5	500	200	500
84		30	500	200	3000
85		200	500	200	10000
86	**E**	10	1000	10	5000
87		10	10000	10	50000
88		1000	10	10	5000
89		10000	10	10	50000
90	**F**	10000	10000	10000	10000
91		5000	5000	5000	5000
92		1000	1000	1000	1000
93		500	500	500	500
94	**G**	10^9	10^9	10^9	10^9
95	**H**	50000	50000	50000	50000
96	**I**	10000	10000	1	1
97	**J**	10	10000	1	1
98	**K**	10000	10	1	1
99	**L**	1	1	1	10000

The 58 Boundary Condition Set for the BGA Benchmark

No		α_{TOP} W/m^{2}K	α_{BOT} W/m^{2}K	α_{SIDE} W/m^{2}K	α_{LEADS} W/m^{2}K
1	**A**	5	1	5	1
2		5	10	5	10
3		5	25	5	50
4		5	50	5	50
5		5	50	5	100
6		5	100	5	200
7		15	1	15	1
8		15	10	15	10
9		15	25	15	50
10		15	50	15	50
11		15	50	15	100
12		15	100	15	200
13	**B**	30	5	30	5
14		30	30	30	30
15		30	50	30	50
16		30	200	30	200
17		80	5	80	5
18		80	30	80	30
19		80	50	80	50
20		80	200	80	200
21		200	5	200	5
22		200	30	200	30
23		200	50	200	50
24		200	200	200	200
25	**C**	25	1	5	1
26		25	10	5	10
27		25	25	5	50
28		25	50	5	50
29		25	50	5	100
30		25	100	5	200
31		75	1	15	1
32		75	10	15	10
33		75	25	15	50
34		75	50	15	50
35		75	50	15	100
36		75	100	15	200
37	**D**	150	5	30	5
38		150	30	30	30
39		150	50	30	50
40		150	200	30	200
41		500	5	200	5
42		500	30	200	30
43		500	50	200	50
44		500	200	200	200
45	**E**	10	50	10	1000
46		10	1000	10	10000
47		1000	5	10	50
48		10000	50	10	500
49	**F**	10000	10000	10000	10000
50		5000	5000	5000	5000
51		1000	1000	1000	1000
52		500	500	500	500
53	**G**	10^9	10^9	10^9	10^9
54	**H**	50000	50000	50000	50000
55	**I**	10000	10000	1	1
56	**J**	10	10000	1	1
57	**K**	10000	10	1	1
58	**L**	1	1	1	10000

A: Free convection
B: Forced convection
C: Heat sink, Free convection
D: Heat sink, Forced convection
E: Cold Plate
F: Fluid Bath
G: Infinite h.t.c.
H: SDJI
I: DCP-1
J: DCP-2
K: DCP-3
L: DCP-4